



## 3D Numerical Modeling of Soft Soil Improved by Rigid Inclusions Supported an Embankment

Messiouid Salah<sup>1</sup>\*, Neghmouche Yassmina

LGCE, Université de Jijel, BP 98 Ouled Aissa, 18000 Jijel, Algérie

\*Corresponding author Email: [smessioud@yahoo.fr](mailto:smessioud@yahoo.fr)

### HIGHLIGHTS

- Numerical modeling of soft soil reinforced by rigid inclusions.
- Calculation of settlements and stresses under the placement of embankment layers
- The settlement at the embankment soil interface has been reduced by 90% compared to a soil without reinforcement.
- Despite the problems encountered with elastoplastic calculations, a good distribution of the stresses in the inclusions is obtained. The charge transfer mechanism is well done for the elementary cell.

### ARTICLE INFO

**Handling editor:** Wasan I. Khalil

**Keywords:** Finite Elements; Rigid Inclusions; Soft Soil; Settlement; Embankment.

### ABSTRACT

A three-dimensional finite element model was suggested to determine the settlements and stresses of an embankment placed on soft soil reinforced by rigid inclusions. To simplify, the layers of soil and the embankment are supposed to be horizontal in a semi-infinite medium, and the base of the soft soil is supposed to be rigid (bedrock). The interacting elements of the model are supposed to be elastic. The determination of the behavior of the soil-inclusions-embankment system was realized according to the construction phases of the embankment layers. The settlements and stresses were calculated according to the construction phases of the embankment layers. The stress and displacement fields are extracted at the end of each calculation phase. The values are then introduced into the model at the beginning of the next phase. The obtained results are presented in terms of the (settlement) vertical displacements and vertical stresses for the elementary cell and the global model, respectively. This study allows the observation of three-dimensional interactions, the load transfer mechanisms and the interaction between the different zones of the embankment. The numerical calculations are much lower than those measured in situ. A verification calculation on the stresses transmitted by the rigid inclusion shows that only 90% of the total load is applied with the numerical calculation.

## 1. Introduction

Reinforcing soft soils with rigid inclusions is an attractive solution based on an economic and technical plan. Their greatest interest lies in a significant reduction in settlement while keeping the soft soil in place, which provides a significant economic and environmental advantage [1-3]. The reinforcement technique by rigid Inclusions consists of setting up a group of Inclusions across the compressible horizon to transfer the charges towards a more rigid horizon. Then, between the group of Inclusions and the Embankment construction, a "load transfer mattress" is intercalated to transmit charges to the inclusions by the vaults formation in the granular soil-forming the Embankment.

The deep foundations and rigid inclusion in the improved soils create a rigid vertical elements group. To understand the behavior of the reinforcement system under the effect of the embankment construction stage, it is important to study the behavior of the rigid inclusions groups. The reinforcement of soft soils by rigid vertical inclusions is a complex problem involving different levels of soil-structure interaction.

The interacting elements are the soft soil, the rigid inclusions, the load transfer mattress, the embankment, and a possible reinforcement nape of Geosynthetics. In such a case, the effects of the soil-inclusion, inclusion-inclusion interaction, mattress or embankment inclusion, and soil-inclusions-mattress embankment interaction under the construction phase of the soil-inclusions-mattress embankment are studied by several researchers, using different methods. The last mentioned is realized by a variety of theoretical methods considered in the literature are based on mechanical elements, such as the load-displacement compatibility method [4], the one-dimensional model [5], or the plane strain models [6-8]. In order to obtain an exact

theoretical solution, the conditions of the compatibility of equilibrium, material behavior, and boundary states must all be satisfied when all the methods have their respective advantages and disadvantages. The complex conditions and the difficulties during the study of the reinforced system with this theoretical method favor using a numerical model because the numerical analysis satisfies all the required conditions and is therefore capable of bringing the exact solution to any geotechnical problem. In this context, many numerical simulations were performed to study the behavior of piled embankments through different numerical methods, such as [2,7, 9-19] and their validity has been regularly confirmed by the scale model results.

Given the complexity of the soil-inclusion-mattress-embankment system and the strong coupling between the interacting elements of the reinforced system, three-dimensional numerical modeling by finite elements is suggested for studying the behavior of the soft soil reinforced by rigid inclusions. The soil, inclusions, transfer mattresses, and embankment layers are integrated into a single calculation. This modeling enabled us to analyze particular aspects of the problem, especially the effect of the embankment construction phases (embankment height) and the influence of rigid inclusion diameter on the reinforcement system behavior. The study of an elementary cell was realized using a non-linear three-dimensional model of the reinforcement system through an elastoplastic behavior law CJS1 (Cambou-Jaffari-Sidoroff). A global three-dimensional model with 30 inclusions is simulated to better understand the load transfer mechanisms. Considering the difficulties of computations with the laws of elasto-plastic behavior, this model realized that the simulations for a continuous medium are perfectly elastic nonlinear. The results are presented and compared with those of elementary cells and the measures in situ.

## 2. Presentation of the numerical study

This section studied three-dimensional numerical modeling in the finite element method of the soil-inclusions system surmounted by an embankment (SIRR) constituted by several layers. The Code-Aster software is used to compute the settlements and stresses under construction phases of the embankment. The inclusions are supposed to be placed on a non-deformable substratum (hard soil layer). The inclusion groups are integrated with a semi-infinite space; the volume elements model soft soil, inclusions, and embankment. The horizontal boundary conditions are placed to prevent the vertical and horizontal movements and to have soil at rest condition. The models were simulated, taking into account the real execution of the rigid inclusions and the embankment placement on the experimental site. The embankment was posed on the soft soil in six layers depending on the mesh Figure configuration 1 and 2.

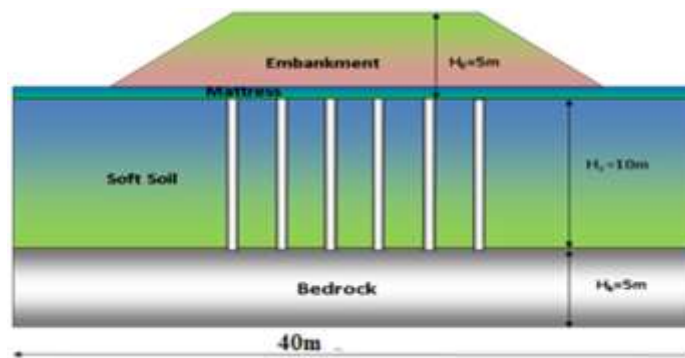


Figure 1: The geometry of the global model (plot of the 30 inclusions)

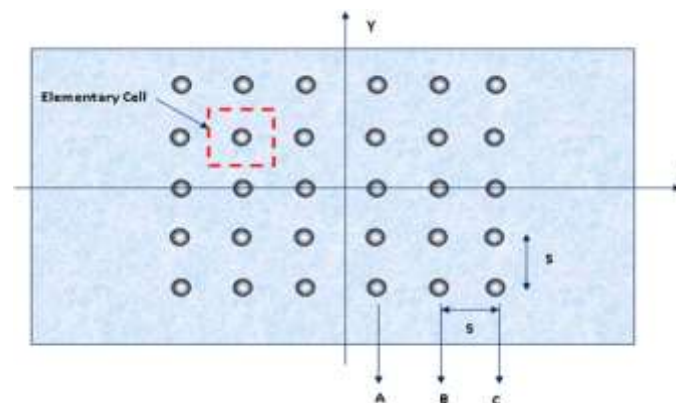


Figure 2: Disposition of the rigid inclusions and elementary cell of numerical modeling

This study is presented in two steps:

The first step presents the study of an elementary cell, including the embankment settlement and the rate of load transfer at the head of a rigid inclusion. The second step shows the inclusions group effect and the load transfer mechanisms of embankment on the rigid inclusions. The number of parameters characterizing this type of structure is very high. Also, based on a realistic configuration, the present study presents the use of a numerical model, which allows a very satisfactory

reproduction of the behavior of granular materials. In this context, several tests on many configurations of the soil-inclusions-Embankment system can be realized. Therefore, this numerical modeling approach is a relevant complement to full-scale experimentation [20]. The objective is to better understand the transfer mechanisms and expenditure involved in the granular mattress and thus bring the practical modalities for the design and dimensions.

The determination of settlements and stresses at the point of rigid inclusion or the embankment under the effect of the construction phases requires, basically, the knowledge of the mechanical properties of the soil through the behavior law. Also, by using the equilibrium equations and the boundary conditions (the shape of the massif, the initial stresses, and the external actions), one can directly obtain the value of the stresses and the settlements by a numerical simulation. It is, therefore, necessary to give an approximate behavior law.

### 3. Presentation of the numerical models

#### 3.1 Geometry and boundary conditions

Only one elementary cell of the reinforced soft soil was analyzed in this section. The calculations are realized under the placement of the embankment layers effect without a load transfer platform. Due to the symmetry conditions, a quarter of the rectangular elementary mesh of  $2\text{m} \times 2\text{m}$  is represented as explained in Figure 3 (i.e., a recovery rate of 2.83%). To simplify the presentation, the soil and embankment layers are supposed to be horizontal in a semi-infinite medium. The soft soil base is supposed to be rigid (hard soil). The characteristics of the interacting elements are presented in Table.1 and Table.2. The Rigid inclusions in the reinforced concrete are about 10 m long; the diameter of these is 0.38 m, and the length-to-diameter ratio is 26.31. The soft soil layer is 10 m high, resting on a hard soil layer of 5m of high Figure 1. The interacting elements are modeled by the volumic elements.

#### 3.2 Elementary cell

The models were simulated, taking into account the real execution of rigid inclusions and the construction phase of the embankment, including the transfer mattress on the experimental site. The embankment was posed on the soft soil in six layers based on the mesh configuration. The phases of the simulations are described below.

Phase 1: Initialization of the stress state in place

Phase 2: Installation of the first layer (Mattress  $h = 0.50$  m)

Phase 3: Installation of the second layer ( $h = 0.50$  m)

Phase 4: Installation of the third layer ( $h = 1.00$  m)

Phase 5: Installation of the fourth layer ( $h = 1.00$  m)

Phase 6: Installation of the fifth layer ( $h = 1.00$  m)

Phase 7: Installation of the sixth layer ( $h = 1.00$  m)

The first phase is the initialization of the stress and displacement field. It consists of the soft horizon and the inclusion, and the implementation of the rigid inclusion is not simulated. At the end of each computation phase, the stress field at the Gauss points and the displacement fields at the nodes are calculated. These values are introduced into the model and introduced in the following phase. In such a case, the loading method is determined according to the characteristics of the embankment layers, the density, the internal friction angle, and the height of each embankment layer. In Code Aster, the Mohr-Coulomb model is replaced by the 1st level of the CJS (Cambou-Jaffari-Sidoroff) model with perfect plasticity (CJS 1) [21]. The mattress, soft soil, and embankment are initially modeled by the behavior model CJS1. The parameters of the CJS can be deduced from the parameters of the Mohr-Coulomb model.

The calculation of the vertical displacements was carried out depending on the height of the embankment layers concerning the 7 phases in the soil-embankment interface along the axis  $xx'$  (the side) and the axis  $yy'$  (the diagonal), as shown in Figure 3.

**Table 1:** Characteristics of the soft soil layers [20]

	<b>H(m)</b>	<b>E(MPa)</b>	<b><math>\nu</math></b>	<b><math>\rho(\text{kg/m}^3)</math></b>	<b>Friction angle</b>
Soft Soil	10	26,50	0,3	2050	20

**Table 2:** Characteristics of the embankment layers [20]

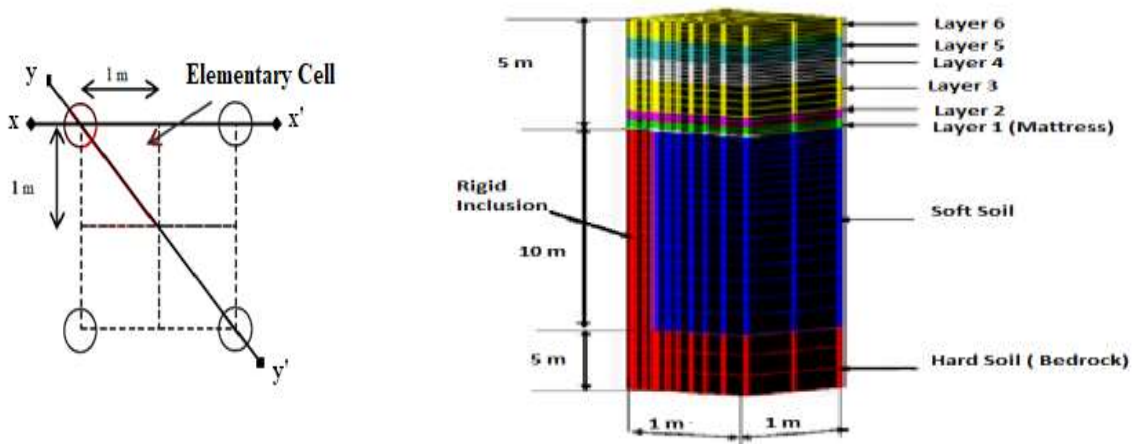
	<b>E (MPa)</b>	<b><math>\nu</math></b>	<b><math>\rho(\text{kg/m}^3)</math></b>	<b>C (KPa)</b>	<b>Friction angle</b>
Embankment layers	70	0.3	1910	17,3	36
Substratum	100	0,2 5	2100	10	35
Mattress	70	0,3	1910	61	36
Rigid Inclusion	18000	0,1	2300	-	-

### 4. Results and discussion

#### 4.1 Settlement study

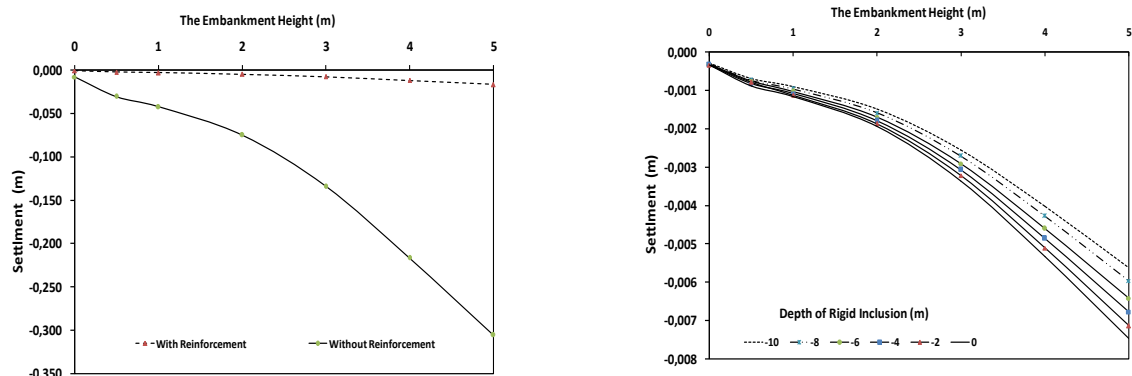
A reference calculation was carried out without reinforcement by rigid inclusions. The results of the settlements of the soft soil without reinforcement and with reinforcement are presented. The soft soil with and without reinforcement is shown and compared in Figure 4. The influence of rigid inclusions in the soft soil on the embankment behavior regarding vertical displacements (settlements) is presented. The numerical results with reinforcement are hardly lower than those without reinforcement, especially for significant embankment heights (the last phase). If the embankment height becomes significant, the displacement becomes major. The displacement of the embankment base for the reinforcement system (SIRR) is much lower than that of the system without reinforcement (SR). Settlement of reinforced and unreinforced soil at the base of the embankment along axis  $xx'$  based on the Embankment Height (Construction Phases)

The Figure shows the influence of the presence of rigid inclusions in the soft soil on the vertical displacement (settlement at the base of the embankment and in the rigid inclusion). A very significant reduction in the vertical settlement of the reinforcement system was noted in Figure 4a. For the reinforced case, the maximum embankment settlement in the  $xx'$  and  $yy'$  is almost 17.6 mm for significant embankment heights (Phase7). On the other hand, the embankment settlement of the unreinforced soil is 306 mm. This shows the main role of rigid inclusions, where a reduction of 90% in the settlement has been observed based on the embankment properties and the soil compressibility. Figure 4b represents the evolution of vertical displacement and rigid inclusion based on the embankment construction phases (embankment height); the obtained results show that the vertical displacement is reduced as a function of the depth of the rigid inclusion for all construction phases. This can be provoked by the friction between the soft soil and the rigid inclusion. The settlement of soft soil is higher than those in the inclusions, which causes negative skin friction around the inclusion shafts and leads to an additional load on the inclusions [22].



a) The geometry of an elementary cell  
 b) 1, 2, 3, 4, 5, and 6: Embankment layers  
 A quarter of an elementary cell model

Figure 3: A quarter numerical model of an elementary cell



a) Comparison between reinforced and unreinforced soil  
 b) Variation of settlement along with the inclusion

Figure 4: Settlement of reinforced and unreinforced soil at the base of the embankment along axis  $xx'$  based on the Embankment Height (Construction Phases)

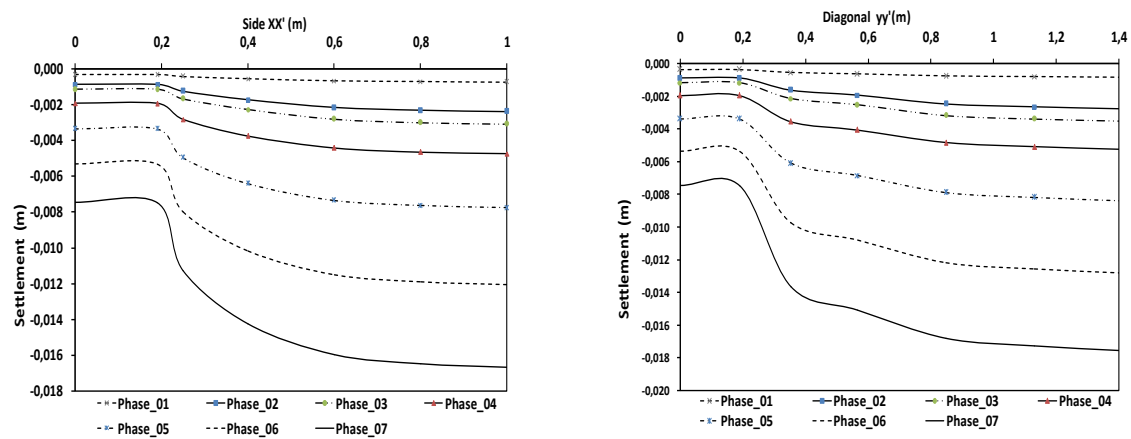


Figure 5: Settlement at the soil- embankment interface on the xx 'and yy' plans

The soil behavior reinforced by rigid inclusions is presented in Figure 5 on the xx 'and yy' plans, respectively. The settlement variation as a function of the placement of the embankment layers (embankment height) has been studied. The settlement of the soft soil in each phase is almost equal on both axes (xx 'and yy'). These figures show that the settlement at the head of the inclusion and the embankment level is strongly affected by the phases of embankment construction (installation of the embankment layers).

Figure 5 shows that the displacement of the head of the inclusion (Origin o) and at the embankment level (planes xx and yy ') is strongly affected by the embankment height. The vertical displacement of the inclusion head is almost less than that of the embankment base. The maximum value in the border of the elementary cell is approximately 17.6 mm (Phase 07); this value is greater than that of the 7.5 mm head of the rigid inclusion. This shows that the embankment is settling faster than the rigid inclusion, and the latter is more stable.

#### 4.2 Stresses study

The stresses are determined by the same construction phases of settlement modeling. The stresses are calculated according to the placement of the embankment layers at the same points as the settlements. The stress calculation was realized in the 7 phases of the embankment construction through the numerical model and especially in the following elements:

- a) The embankment foundation (soft soil surface):
  - According to axis xx '(the side).
  - Along the yy 'axis (the diagonal).

The role of inclusions is to reduce the settlement of soft soil and ensure the good transmission of the vertical loads to a more rigid support layer without touching the soft soil layer.

The transmission operation of the vertical load towards the rigid inclusions is presented in Figure 6; this is devoted to the presentation of the variety of the stresses as a function of the placement of embankment layers in accordance with the two plans xx 'and yy.' The stress values are maximal at the head of the rigid inclusion and lower in the soil-embankment interface with two plans (xx 'and yy'). The obtained results show the effectiveness of the reinforcement system. The majority of the piled embankment is supported by rigid inclusion. Figure 6 shows that the transfer of charge by inclusion is done in a real correct manner. The stress on the soft soil is much lower than the part of the transferred load to the head of the rigid inclusion.

#### 4.3 Influence of the rigid inclusion diameter on the stress variation

Diameter is an important parameter for dimensioning the reinforcement system. Their influence is on the load transfer rate, i.e., it increases the strength of the rigid inclusion.

Figure 7 presents the effect of the rigid inclusion diameter on the variation of the vertical stresses based on the planes xx 'and yy', respectively. The obtained results are similar to those presented in Figure 6. The numerical results show that the stresses in the rigid inclusion are reduced due to the increase in diameter (increase in recovery rate). For larger diameters, the entire embankment load can be supported by the inclusion. The influence of the increase of the diameter on the load transfer has been shown by the increase in the grip surface of the rigid inclusions.

Figure 8 shows the influence of the inclusion diameter on the settlement under the effect of the placement of the sixth layer of embankment (embankment construction phase or embankment height). The obtained results show that the settlement at the head of the inclusion and the embankment base (the plans xx' and yy' respectively) are significantly reduced due to the increase of the rigid inclusion diameter.

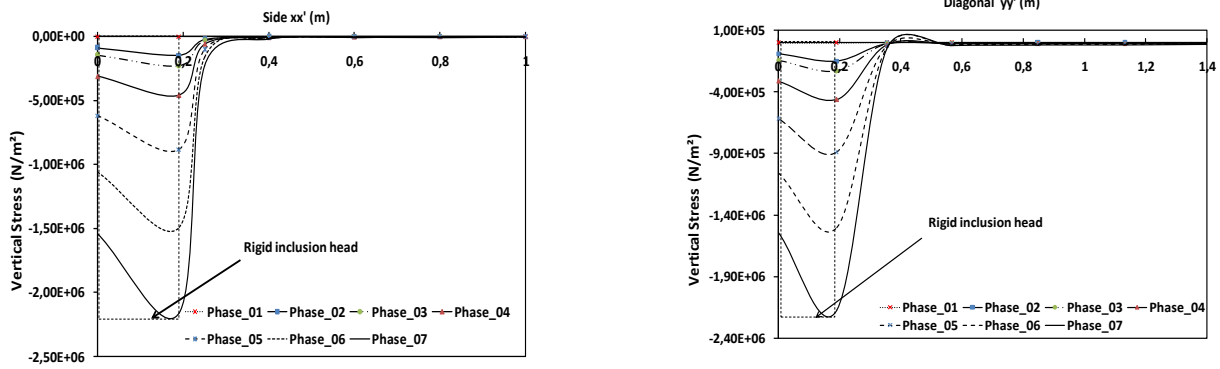


Figure 6: Vertical constraints at the soil-embankment the yy' and xx' planes

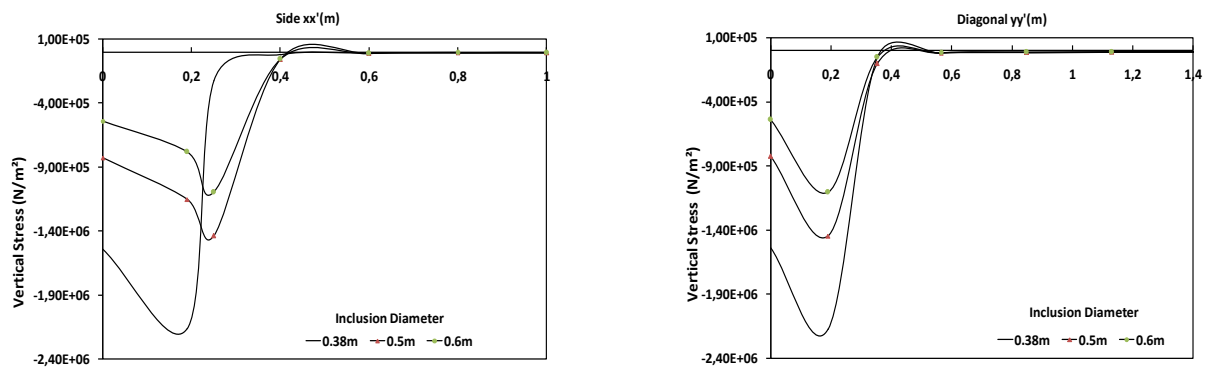


Figure 7: The effect of the rigid inclusion diameter on the variation of the embankment stresses in the xx' and yy' planes

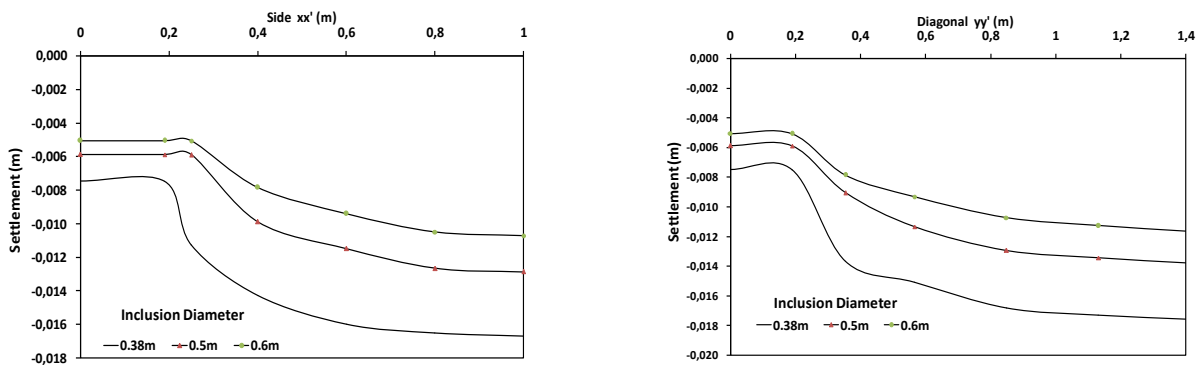


Figure 8: Settlement according to the diameter of the rigid inclusion on the xx' and yy' plans.

### 5. Numerical modeling of global system soil-inclusions-embankment

To better understand the load transfer mechanisms, the group effect, and the influence of the symmetry in reinforcement under the embankment construction phases, a global three-dimensional model with 30 inclusions is simulated. Taking into account the difficulties of computations with the laws of elasto-plastic behavior, the simulations were realized for a continuous medium perfectly elastic nonlinear. The objective of these simulations is to examine the overall behavior of a plot of 30 rigid inclusions. In this section, the calculations of the settlements and the stresses are addressed according to the same procedure presented in the study of the elementary cell. The vertical stresses and the settlements are calculated by a quarter model. The embankment layers with the same thickness of 1m are placed successively on a load distribution mattress of the elasticity module 50.106 (Pa). The rigid inclusions are 0.38m in diameter with a spacing of 2 m and are introduced into the soft soil layer spanning to 10 m and placed on a rigid layer of 5 m.

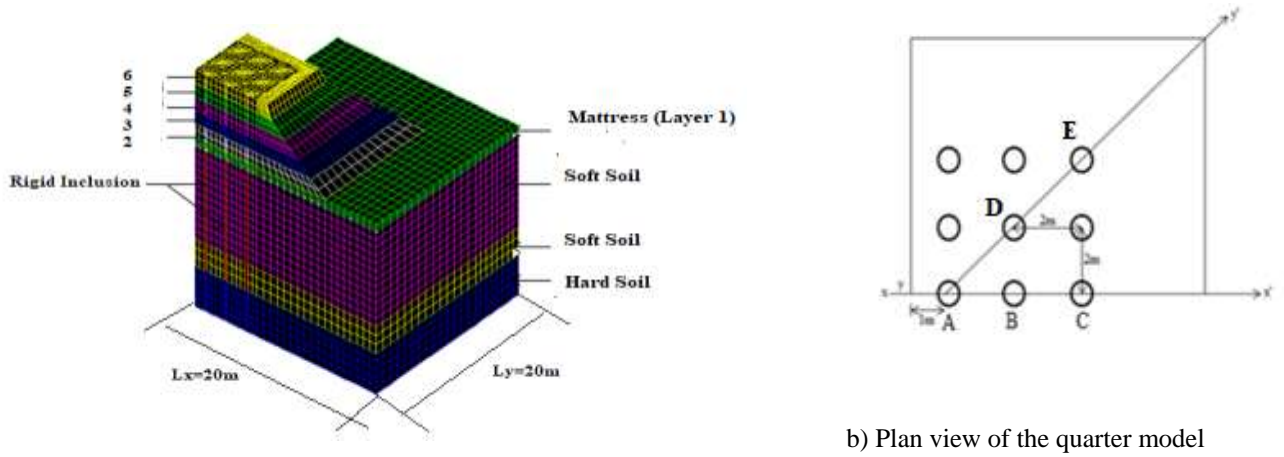


Figure 9: A numerical model for calculating the rigid inclusion groups [23]

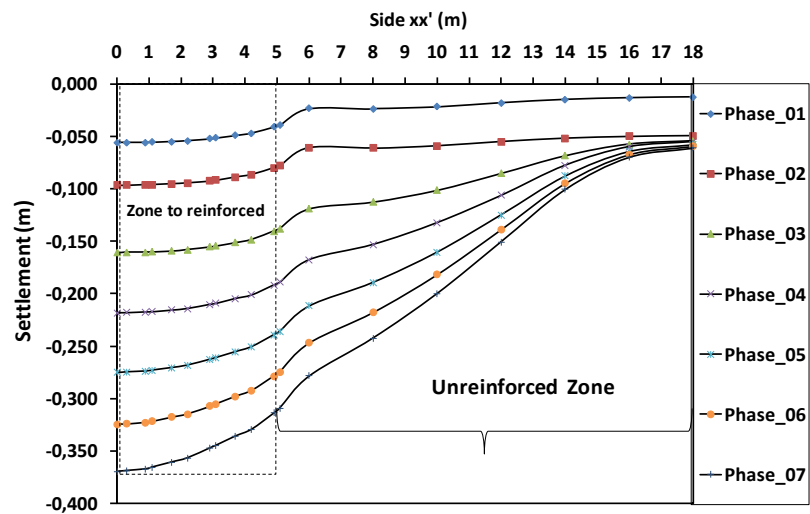


Figure 10: Settlement in the embankment base along xx'. - Unreinforced Case-

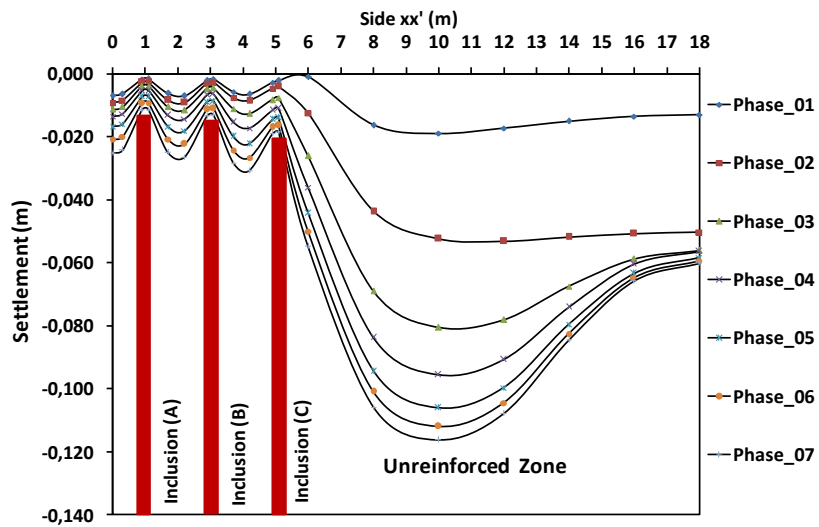


Figure 11: Settlement in the embankment base along xx'. - Reinforced Case-

Figures 10 and 12 clearly show baseline results for an unreinforced system. The calculation was carried out through the same steps of the embankment construction. The obtained results confirm the need for reinforcement of soft soil and, at the same time, bring an idea for the settlement of embankment without reinforcement, and the maximum settlement is 350 mm. Figures 11 and 13 show the settlement variation in the soft soil surface (embankment base). For all construction phases of the embankment layers, the displacement at the level of the heads of inclusions is less than that at the floor of the embankment. However, the settlement of the head of the rigid corner inclusion is greater than that of the intermediate rigid inclusions. The difference between the reinforced and unreinforced parts of the soft soil is very remarkable on the  $xx'$  and  $yy'$  axis. A maximum settlement of 116 mm is obtained in the center of the embankment on the unreinforced soil.

With the same set of parameters, the maximum settlement of the global model is greater than that of the elementary cell; this expected difference is explained by the group effect. The elementary cell refers to the case of an infinite soil reinforced by rigid inclusions. For reinforced soil, the maximum settlement is 30.8 mm below the slope. There is also a gradual increase in settlement under the unreinforced part of the embankment.

The unreinforced part cup faster 120mm and packed the reinforced part. The stresses on the rigid inclusion heads increase as one approaches the unreinforced slope. Because the par soft soil under the slope is not reinforced by the rigid inclusions, it is very important to consider this interaction when comparing the in situ results with the simulations of an elementary cell presented below. The global model allows the observation of three-dimensional interactions, the load transfer mechanisms, and the interaction between the different embankment zones. The obtained results presented in Figures 14 and 15 show the influence of the inclusion diameter on the settlement in the rigid inclusions and the unreinforced part. The settlements are reduced as a function of the increase in the diameter of the inclusions. It is noted that the diameter significantly influences the reinforcement system.

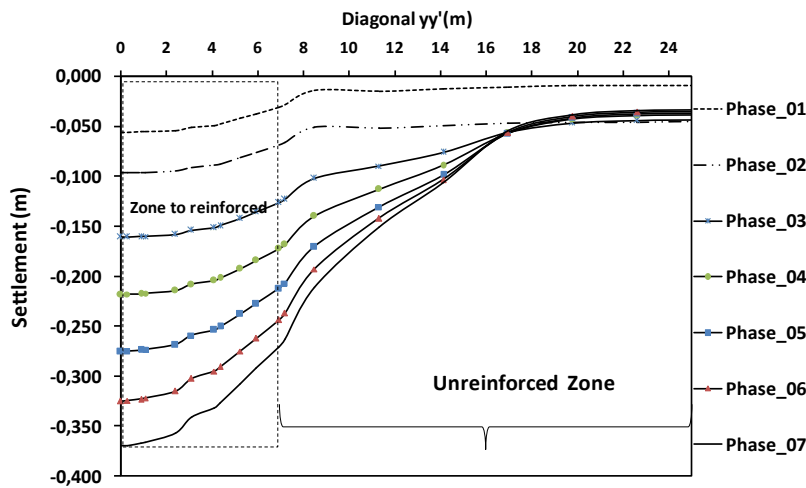


Figure 12: Settlement in the embankment base along  $yy'$ . - Unreinforced Case-.

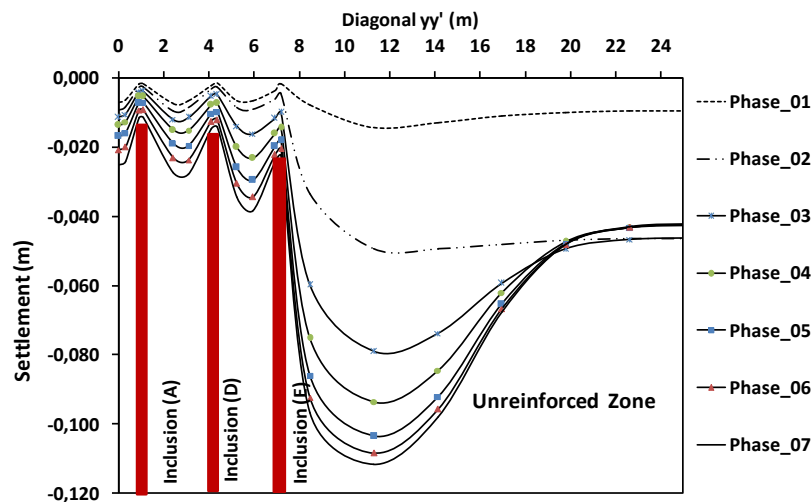


Figure 13: Settlement in the embankment base along  $yy'$ . - Reinforced Case-.



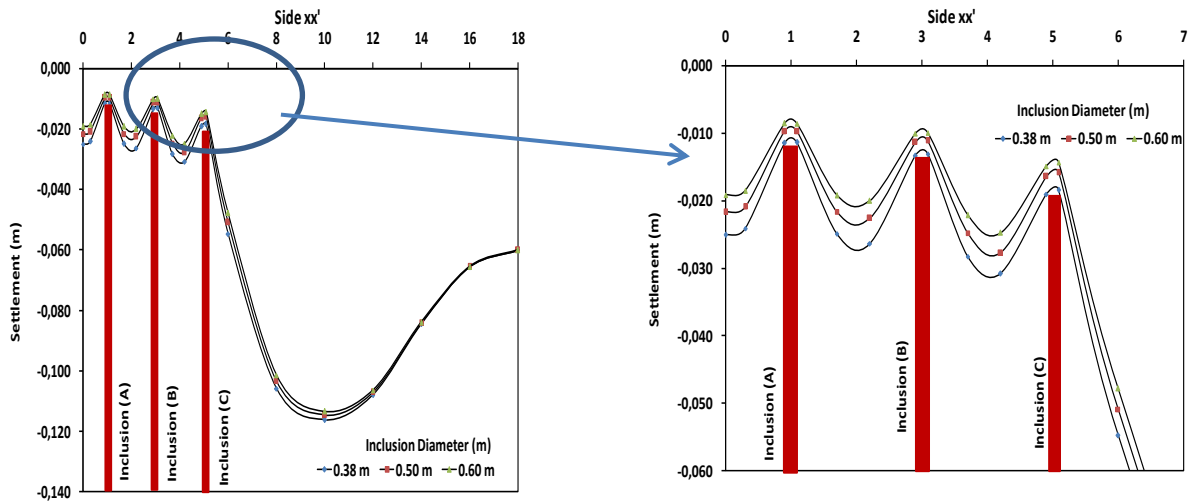


Figure 14: Settlement of phase 07 as a function of the diameter of the inclusion along the axis  $xx'$

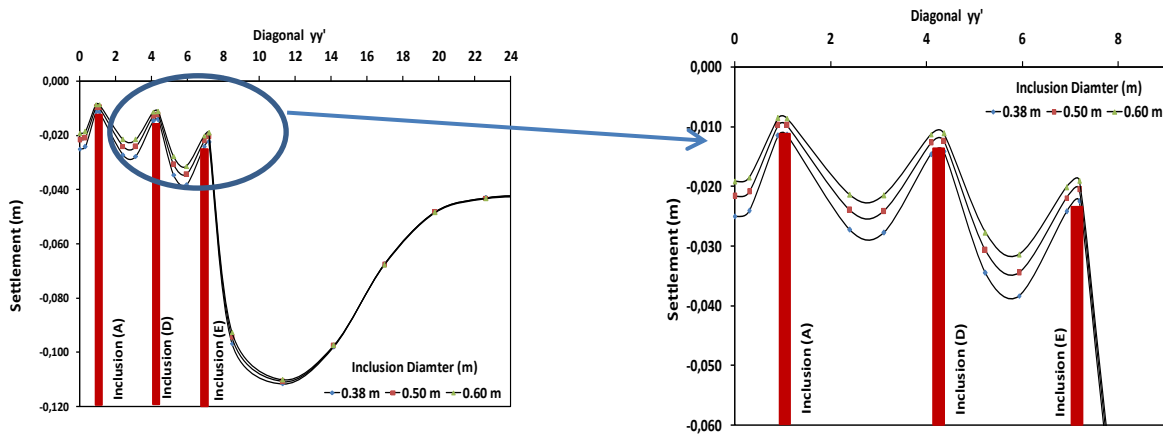


Figure 15: Settlement of phase 07 as a function of the diameter of the inclusion along the axis  $yy'$

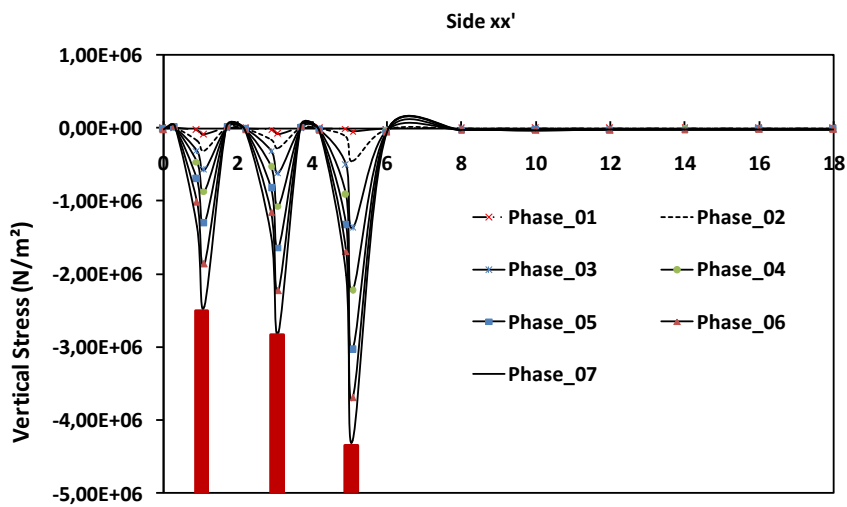


Figure 16: Vertical stresses at the level of the embankment along the axis  $xx'$

Figures 16 and 17 show the variation of the vertical stresses on the axis  $xx'$  and  $yy'$  of the global model at the embankment base. The stresses on the soft soil surface are lower than those transferred to the rigid inclusions, so the load transfer is performed to the rigid inclusions. In contrast, in rigid inclusions under the slope, the stress calculated at the head of inclusion C is greater than the stress calculated at the head of inclusions A and B. The stress on inclusion C before the unreinforced slope is twice the size of that of the previous inclusion because the unreinforced slope causes part of the load.

The stresses in the three inclusions are strongly affected by the embankment load and the soil thrust effect of the unreinforced part. A good concentration of the stresses on the inclusions is observed. This shows the good functioning of the rigid inclusions and the reinforcement system. The mattress plays an important role as the load transfer platform where the soil arches are formed. The efficacy, which is defined as the proportion of the total load applied to the rigid inclusions, is usually used to assess the load-bearing capacity of the system.

### 6. Comparison of the numerical results with the measurements results

The experimental instrumentations are presented in the Briancon report 2.08.1.05. It measures the load transfer, the vertical displacements of the rigid inclusions and soil, the variation of the pore-water pressure, the deformations of rigid inclusions and geosynthetic, and the lateral displacements of the soil the inclination of the rigid inclusions at the foot of the slope. The measurements were made at the beginning of the implementation of the embankment. The report 2.08.1.05 [20], submitted to PN ASIRI, presents the measurements results of the Chelles site. The Vertical stresses are measured at several points with the circular total pressure sensors. They are placed at the head of the inclusion and between the mesh in different places in the mattress. The location of the pressure sensors is presented in Figure 20. The Settlement of the inclusion heads, the soil at the base of the embankment, and the reinforced system's load transfer platform were measured using transducers. These transducers were installed in accordance with the plan shown in Figure 20. The results of the numerical calculations were compared with the in situ measurements are presented. Figures 21 and 22 compare the reinforced system's settlements and vertical stresses. The Figure shows that the numerical calculations' settlements are much lower than those measured in situ. A verification calculation of the stresses transmitted by the rigid inclusion shows that only 90% of the total load is applied to the numerical calculation.

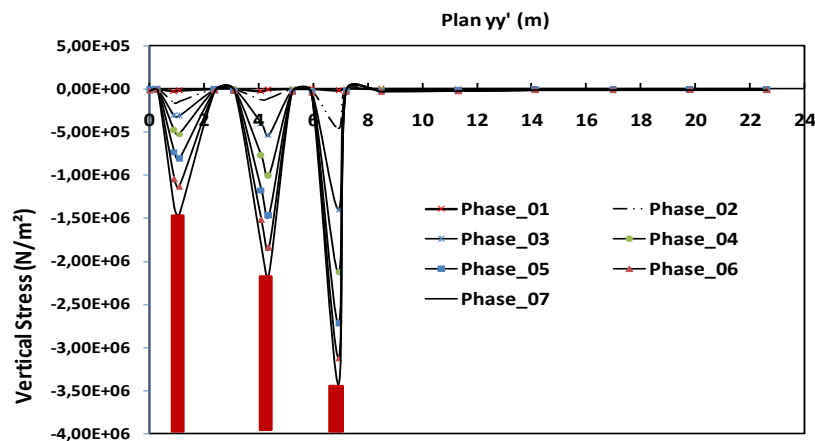


Figure 17: Vertical stresses at the level of the embankment along the axis  $yy'$ .

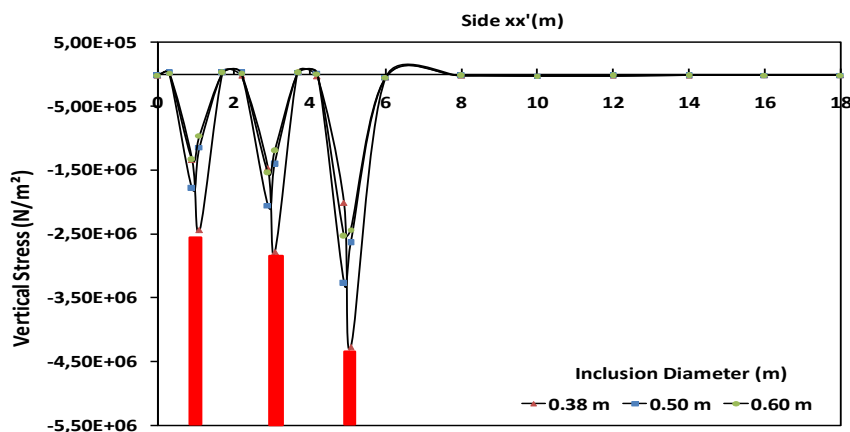


Figure 18: Vertical stresses as a function of the inclusion diameter along the axis  $xx'$ .

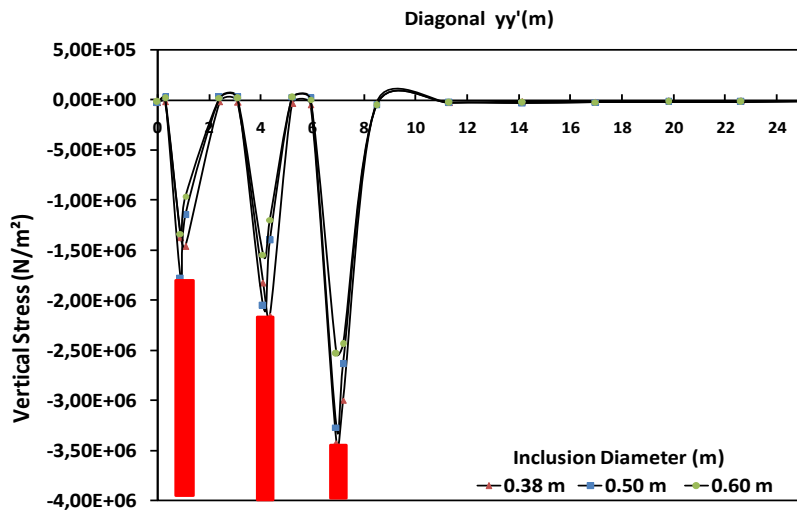
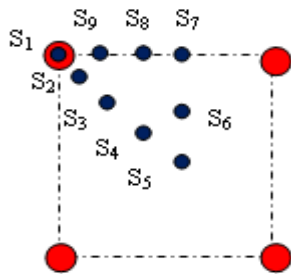
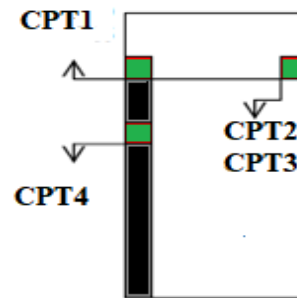


Figure 19: Vertical stresses as a function of the diameter inclusion along the axis  $yy'$ .



Disposition of the Transducer sensors



Disposition of the Circular total pressure sensors

Figure 20: Disposition of the sensors at the head of rigid inclusions and in the mesh

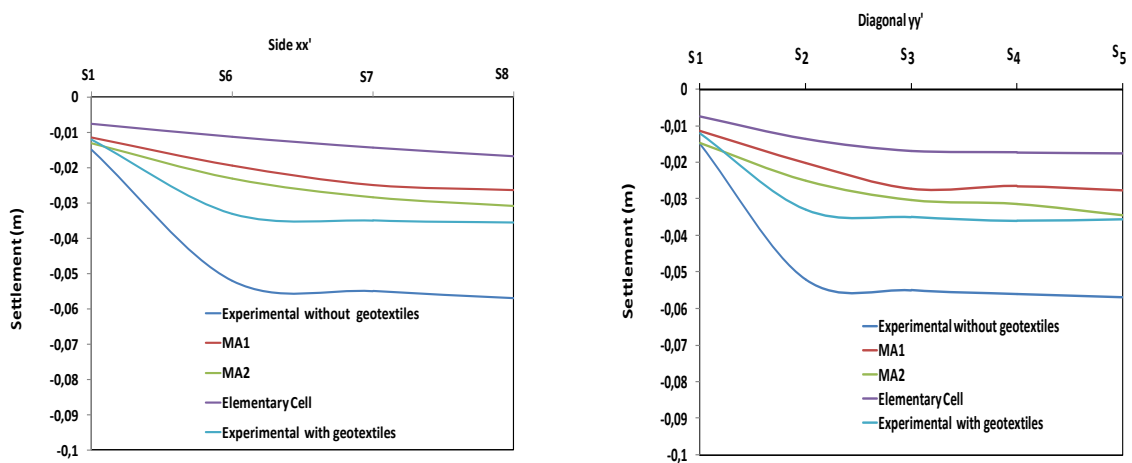


Figure 21: Comparison of numerical results with in situ measurements (Settlement)

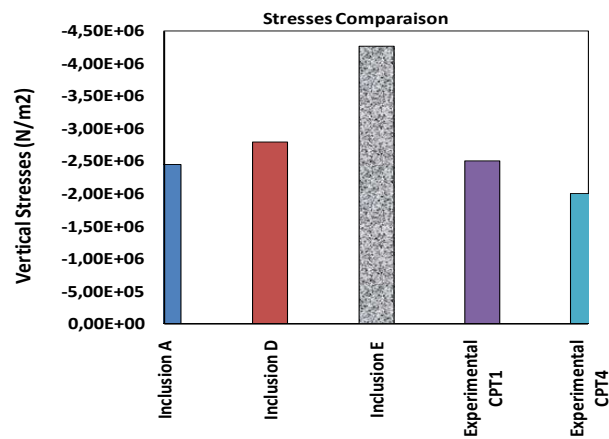


Figure 22: Comparison of numerical results with in situ measurements (stresses)

## 7. Conclusion

This work presents a study of the behavior of soft soil reinforced by rigid inclusions surmounted by an embankment, using three-dimensional numerical modeling of the interaction between soil, inclusions, and the embankment. It makes it possible to calculate the settlements and stresses in the rigid inclusions, at the level of embankments and the reinforced soil for an elementary cell and a group of inclusions (three-dimensional global model) under the effect of the construction phases of embankments. The mesh of the numerical models is realized by the Castem software, and the simulations are realized by Code aster 13.2.

The software Aster Code is used for computing, settlements, and stresses under the construction phase of the embankment. The inclusions are assumed to be placed on a non-deformable substratum (hard soil layer). The interacting elements are elastoplastic, and a CJS1 (Cambou-Jaffari-Sidoroff) behavior law has been applied to study the charge transfer. The obtained results of the numerical simulation of the elementary cell show the correct functioning of the reinforcement system.

-The maximum stresses at the base of the support layer obtained on the side and the diagonal are almost zero. The settlement on the soft soil surface for the elementary cell is approximately 306 mm of the unreinforced soil. For the soil reinforced by rigid inclusions, a 90% reduction in embankment settlement was noted.

-The stress analysis shows that the entire embankment load is almost transmitted to the rigid inclusions. Despite the problems encountered with elastoplastic calculations, a good distribution of the stresses in the inclusions is obtained. The charge transfer mechanism is well done in the elementary cell.

-For the group effects, the maximum settlement of the global model is greater than that of the elementary cell (350 mm); this expected difference is explained by the group effect and the unreinforced part. The elementary cell corresponds to the case of an infinite soil reinforced by rigid inclusions.

-The unreinforced part cup faster 120mm and packed the reinforced part. As a result, the stresses on the rigid inclusion heads increase as one approaches the unreinforced slope. Therefore, it is very important to take this interaction into account when comparing the in situ results with the simulations of an elementary cell presented below.

-The diameter of the rigid inclusions plays a very important role, including reducing settlements (increases the grip surface). Therefore, the results of this study allow putting the effect of diameter and the effect of the rigid inclusions groups.

-The settlements obtained by the numerical calculations are much lower than those measured in situ.

Finally, this three-dimensional model shows the influence of the unreinforced zone on the behavior of the rigid inclusions under the embankment. It is important to take into account the influence of the unreinforced part of the embankment on the stress distribution and the settlement profile on the compressible soil when comparing the in situ results with simulations of an elementary cell. These observations are consistent with those of the full-scale experiment. Using constitutive laws more suited to the geomaterials in place will allow for a better qualitative agreement between the experimental results and the numerical results.

### Author contribution

All authors contributed equally to this work.

### Funding

This research received no specific grant from any funding agency in the public, commercial, or not-for-profit sectors.

### Data availability statement

The data that support the findings of this study are available on request from the corresponding author.

### Conflicts of interest

The authors declare that there is no conflict of interest.

## References

- [1] L. Briancon, R. Kastner, B. Simon, D. Dias, Etat des connaissances - Amlioration des sols par inclusions rigides. Symp. Int. sur l'Amlioration des Sols en Place. ASEP-GI, 9-10 septembre 2004, Paris, Presses de l'Ecole Nationale des Ponts et Chausses, (2004) 15-44.
- [2] O. Jenck, D. Dias, R. Kastner, Two Dimensional Physical and Numerical Modelling of a Pile-Supported Earth Platform over Soft Soil, *J. Geotech. Geoenviron. Eng.*, 133 (2007) 295-305. [https://doi.org/10.1061/\(ASCE\)1090-0241\(2007\)133:3\(295\)](https://doi.org/10.1061/(ASCE)1090-0241(2007)133:3(295))
- [3] Simon B., Schlosser F. State of the Art, Soil reinforcement by vertical stiff inclusions in France, in: SYMPOSIUM Rigid Inclusions in Difficult Subsoil Conditions. Mexico City, 2006.
- [4] B. FitzPatrick, R. Gernant, J. Miceli, Design and construction of intermediate foundation solutions for wind turbines, In Contemporary topics in deep foundations, [https://doi.org/10.1061/41021\(335\)63](https://doi.org/10.1061/41021(335)63)
- [5] R. P. Chen, Y. M. Chen, J. Han, and Z. Z. Xu, A theoretical solution for pile-supported embankments on soft soils under one-dimensional compression, *Can. Geotech. J.*, 45 (2008) 611-623. <https://doi.org/10.1139/T08-003>
- [6] K. Deb, A mathematical model to study the soil arching effect in stone column-supported embankment resting on soft foundation soil, *Appl. Math. Modell.* 34 (2010) 3871-3883. <https://doi.org/10.1016/j.apm.2010.03.026>
- [7] L. Zhang, M. Zhao, Y. Hu, H. Zhao, and B. Chen, Semi-analytical solutions for geosynthetic-reinforced and pile-supported embankment, *Comput. Geotech.*, 44 (2012) 167-175. <https://doi.org/10.1016/j.compgeo.2012.04.001>
- [8] K. Deb, and S. R. Mohapatra, Analysis of stone column-supported geosynthetic-reinforced embankments, *Appl. Math. Modell.*, 37 (2013) 2943-2960. <https://doi.org/10.1016/j.apm.2012.07.002>
- [9] P. Mestat, Bourgeois, E., and Riou, Y. Numerical, modelling of embankments and underground works, *Comput. Geotech.*, 31 (2004) 227-236. <https://doi.org/10.1016/j.compgeo.2004.01.003>
- [10] N. Mattson, A. Menoret, C. Simon, and M. Ray, Case study of a full-scale load test of a piled raft with an interposed layer for a nuclear storage facility, *Gotechnique*, 63 (2013) 965-976. <https://doi.org/10.1680/geot.12.P.166>
- [11] J. Han, and M. Gabr, Numerical Analysis of Geosynthetic-Reinforced and Pile-Supported Earth Platforms over Soft Soil, *J. Geotech. Geoenviron. Eng.*, 128 (2002) 44- 53. [https://doi.org/10.1061/\(ASCE\)1090-0241\(2002\)128:1\(44\)](https://doi.org/10.1061/(ASCE)1090-0241(2002)128:1(44))
- [12] O. Jenck, D. Dias, R. Kastner, Three-dimensional numerical modeling of a piled embankment, *J. Geotech. Geoenviron. Eng.*, 9 (2009) 102- 112. [https://doi.org/10.1061/\(ASCE\)1532-3641\(2009\)9:3\(102\)](https://doi.org/10.1061/(ASCE)1532-3641(2009)9:3(102))
- [13] Naughton, P.J. The significance of critical height in the design of piled embankment, *Soil Improvement, Geo-Denver*, 2007. [https://doi.org/10.1061/40916\(235\)3](https://doi.org/10.1061/40916(235)3)
- [14] D. Dias, B. Simon, Spread foundations on rigid inclusions subjected to complex loading: Comparison of 3D numerical and simplified analytical modeling, *Am. J. Appl. Sci.*, 12 (2015) 533-541.
- [15] P. Burtin, J. Racinais, Embankment on Soft Soil Reinforced by CMC Semi-Rigid Inclusions for the High-speed Railway SEA, *Procedia Eng.*, 143 (2016) 355-362. <https://doi.org/10.1016/j.proeng.2016.06.045>
- [16] Racinais, J. and Plomteux, C. Design of slab-on-grades supported with soil reinforced by rigid inclusions. Retrieved from EYGEC 2011, Rotterdam, (The Netherlands), 2011. <https://doi.org/10.3233/978-1-60750-808-3-105>
- [17] H. Liu, W. Charles, K. Fei, Performance of a geogrid-reinforced and pile-supported highway embankment over soft clay: Case study, *J. Geotech. Geoenviron. Eng.*, 133 (2007) 1483-1493. [https://doi.org/10.1061/\(ASCE\)1090-0241\(2007\)133:12\(1483\)](https://doi.org/10.1061/(ASCE)1090-0241(2007)133:12(1483))
- [18] Y. Zhuang, and K. Wang, Finite-element analysis on the effect of subsoil in reinforced piled embankments and comparison with theoretical method predictions, *Int. J. Geomech.*, 16 (2016) 04016011. [https://doi.org/10.1061/\(ASCE\)GM.1943-5622.0000628](https://doi.org/10.1061/(ASCE)GM.1943-5622.0000628)
- [19] M. Y. Fattah, H. A. Mohammed, H. A. Hassan, Load transfer and arching analysis in reinforced embankment, *Proc. Inst. Civ. Eng. Struct. Build.*, 169 (2016) 797-808. <https://doi.org/10.1680/jstbu.15.00046>
- [20] Briancon L., Rapport N 2.08.1.05. A.S.I.R.I. - Tranche 2 - Thme 1 : rapport final. CNAM. (2008)
- [21] B. Cambou, K. Jafari, Modle de comportement des sols non cohrents, *Rev. Fr. Geotech.*, 44 (1988) 43-55. <https://doi.org/10.1051/geotech/1988044043>
- [22] Smith, M.E. Design of bridging layers in geosynthetic-reinforced column-supported embankments. PhD thesis, Department of Civil and Environmental Engineering, Virginia Polytechnic Institute and State University, 2005.
- [23] S. Messioud, U. S. Okyay, B. Sbartaı, D. Dias, Dynamic response of pile reinforced soils and piled foundations. *Geotech, Geol. Eng.*, 34 (2016) 789-805. <https://doi.org/10.1007/s10706-016-0003-0>